

Optical Properties of Silver nanocrystals Self-Organized in 2D superlattice : Substrate Effect

N. Pinna, M. Maillard, A. Courty, V. Russier, and M. P. Pileni*

*Laboratoire des Matériaux Mésooscopiques et Nanométriques, URA CNRS 7070
Université Pierre et Marie Curie, BP 52,
4 Place Jussieu, 75005 Paris, France*

Abstract

Experimental and calculated reflectivity spectra of silver nanocrystals self-assembled in compact hexagonal networks on various substrates (HOPG, gold, silicon and $\text{Al}_{0.7}\text{Ga}_{0.3}\text{As}$) are compared. The calculated spectra are deduced from a model based on a mean field theory and taking into account the electromagnetic resonances for p (parallel) and s (perpendicular) polarizations. From experimental and calculated spectra, it is concluded that the major change in the responses is due to the refractive index of the substrate. Hence, the optical properties of coated silver nanocrystals organized in a hexagonal network do not depend on the substrate used. That is to say no specific interactions between nanocrystals and substrate take place. Collective optical properties due to the formation of a film made of 5-nm silver nanocrystals are observed. This is pointed out by the appearance of an additional resonance at a higher energy than that of the plasmon resonance of isolated nanocrystals.

I. INTRODUCTION

After nearly a decade, the study of optical properties of silver nanoparticles is still attractive for a large number of scientists because many problems are not yet solved. However some behaviors are already well known. For example, the surface plasmon resonance excitations of spherical silver nanoparticles dispersed in a matrix are in UV-Visible range¹. They are size dependent, the bandwidth increases with decreasing particle size². The surface plasmon resonances are strongly influenced by their environments and depend on the dielectric functions of the surrounding^{2,3} medium. A marked broadening of the surface plasmon resonance is observed when the nanoparticles are embedded with "reactive" matrices such as CO, C₂H₄, C_nH_{2n+1}SH as compared with an "inert" matrix such Ar^{2,4-6}.

Very recently, it was found that on decreasing the particle size the optical properties of single silver nanoparticles deposited on alumina by vapor deposition show a drastic change in the resonance position with a shift to higher energies and an increase in the linewidth. This reflects the growing importance of the quantum size effect⁷. The same group demonstrated that the substrate has a drastic effect on the electronic properties of gold nanoparticles⁸.

A large number of measurements and theoretical models for 2D systems made of silver nanoparticles have been published⁹⁻¹⁶. In most of the results, the major modifications of the optical properties of silver nanoparticles are due to the particle-particle and particle-substrate interactions. The optical properties of nanoparticles deposited on a surface were also strongly modified. This effect was mainly attributed to image forces induced in the substrate by the nanoparticles in close contact^{12,16,17}.

In the last few years we demonstrated, experimentally, that it is possible to self organize coated silver nanocrystals in compact hexagonal networks¹⁸. Such 2D superlattices exhibit optical collective properties¹⁹⁻²¹. With silver nanocrystals, by reflectivity²¹, under polarized light, two plasmon resonances, characteristic of the optical anisotropy were observed. As previously seen, when the nanoparticles are in contact with the surface, the substrate plays an important role in the optical properties, a question then arises: Do the optical properties of our coated nanocrystals self organized on a surface and not in contact with the surface, change with the substrate used? In the present paper we answer this question.

To determine the substrate influence on the optical properties of coated silver nanocrystals self organized in a hexagonal network, experimental reflectivity spectra of 5-nm silver nanocrystal

monolayers deposited on various substrates are modeled.

II. EXPERIMENTAL SETUP

The optical reflectivity spectra of 5-nm silver nanocrystal monolayers are measured with a double monochromator recording spectrophotometer (Model Varian Cary 5) equipped with rotational stages for angular measurements and polarizers (VASRA). The energy range is 2 - 4.5 eV. The light is polarized either perpendicular (s) or parallel (p) to the incidence plane and the incidence angles range from 20° to 60° with respect to the normal to the surface. Under s-polarization, the electric field vector is always directed along the particle film (parallel to the substrate). This tends to be insensitive to plasmon modes oriented perpendicular to the substrate and does not provide any information on the optical surface anisotropy. Conversely, under p-polarization, the electric field has two components: one is perpendicular to the particle film and grows with increasing θ , the other is parallel to the film and decreases with increasing θ . Hence, the (p) polarization provides information on the optical film anisotropy. To ascertain if there are several resonance peaks, the reflective spectra under polarized light perpendicular (s) or parallel (p) to the incidence plane at various incidence angles, θ are recorded. R and R_0 are the reflectivities of the system containing or not a monolayer formed by 5-nm silver nanocrystals. The reflectivities under p polarization at 60° incidence angle of the various bare substrates are in Figure 1. They clearly differ with the substrate used. With HOPG, the reflectivity is constant (10 %) from 2 eV to 3.5 eV and then increases. With gold, it is very high at low energy. It markedly decreases with increasing energy to reach a constant value above 2.6 eV (17 %). With silicon, it increases between 2 eV (13 %) and 4.5 eV (60 %). A shoulder around 3.4 eV is observed. With $\text{Al}_{0.7}\text{Ga}_{0.3}\text{As}$, it increases between 2 eV (10 %) and 4.5 eV (30 %) with a shoulder around 3.5 eV.

III. MODEL

To understand the experimental spectra and to determine clearly the positions of the plasmon resonances, the reflectivity spectrum of this system has been calculated. We have modeled it in three steps:

- i) The dielectric function of isolated silver nanocrystals is calculated by a Drude-like approximation²², which takes into account the presence of the d-electrons.

ii) The monolayer is modeled as a homogeneous film made of 5-nm silver nanocrystals with a nearest neighbor distance of 7 nm in a medium of dielectric constant $\varepsilon = (2.0)$ corresponding to the dielectric constant of thiododecane in the UV-Visible wavelength range. The minimal distance between particle centers is measured experimentally (7 nm) by using the TEM image. The effective dielectric function of the nanocrystal film is deduced from a slight modification of the theory developed by Barrera et al.¹⁴. In the present case, we assume there is one nanocrystal monolayer in a surrounding medium of dielectric constant, ε_m .

The effective nanocrystal film polarization is assumed to be that of the overall nanocrystals forming the film and organized in a compact hexagonal network. It is characterized by an anisotropic dielectric function $(\varepsilon_p^x, \varepsilon_p^z)$ in an infinite surrounding medium of dielectric constant ε_m . Thus the dielectric function obtained coincide with ε_p ($\varepsilon_{eff}^x = \varepsilon_p^x$ and $\varepsilon_{eff}^z = \varepsilon_p^z$). The obtained formulas are:

$$\frac{\varepsilon_{eff}^x}{\varepsilon_m} = \frac{1 - (\lambda\tilde{\alpha}/8)(S_0/2) + 2\gamma(2a/d)^2\tilde{\alpha}}{1 - (\lambda\tilde{\alpha}/8)(S_0/2)} \quad (1a)$$

$$\frac{\varepsilon_{eff}^z}{\varepsilon_m} = \frac{1 + (\lambda\tilde{\alpha}/8)S_0}{1 + (\lambda\tilde{\alpha}/8)S_0 - 2\gamma(2a/d)^2\tilde{\alpha}} \quad (1b)$$

with a the radius of the nanocrystals, d the nearest neighbor distance, $f_s = (\pi/2\sqrt{3})(2a/d)^2$ the surface fraction occupied by the nanocrystals, $\gamma = f_s/(2a/d)^2$, $\lambda = (2a/d)^3$, $\tilde{\alpha} = \frac{\varepsilon_s(\omega) - \varepsilon_m}{\varepsilon_s(\omega) + 2\varepsilon_m}$. $S_0 = \sum_j \frac{1}{(r_{ij}/d)^3}$ is the reduced value of the projection, in the direction normal to the surface, of the dipolar fields. For a hexagonal lattice $S_0 = 11.034$.

iii) The whole system is modeled (Fig. 2) by a stratified medium composed of

- a) 2-nm layer of thiododecane.
- b) 5-nm layer of silver nanocrystals calculated from ii).
- c) 2-nm layer of thiododecane and the substrate.

The dielectric function of the substrates is taken from Palik's handbook²³. The reflectivity spectrum is then calculated by a matrix method from Abelès theory of stratified media^{24,25}. In this method each layer is characterized by a matrix that take into account its dielectric function and its thickness.

IV. SILVER NANOCRYSTALS ASSEMBLED IN 2D AND 3D

5-nm silver nanocrystals are synthesized by the reverse micelle technique described previously^{26,27}. They are coated with dodecanethiol molecules, extracted from the micellar solution and then dispersed in hexane¹⁸. One drop of a low concentration silver nanocrystal solution is deposited on the HOPG substrate in order to form a monolayer. After solvent evaporation, a monolayer of nanocrystals organized in a hexagonal compact structure (Fig. 3A) is formed¹⁸. On replacing HOPG by a gold substrate, the STM image clearly shows a film of close-packed nanocrystals (Fig. 3B). With silicon, the high resolution SEM (scattering electron microscopy) image shows that the nanocrystals keep similar organization as HOPG (Fig. 3C). With $\text{Al}_{0.7}\text{Ga}_{0.3}\text{As}$, it has been impossible to produce a direct image of a monolayer formed because of lack of equipment.

To demonstrate that compact monolayers made of 5-nm nanocrystals are formed, "supra" crystals were built up. Let us first recall what has been already obtained with HOPG substrates. On increasing the silver nanocrystal concentration ($[\text{Ag}_n] = 3.10^{-6}$ mol/l), large "supra" crystals are fabricated. It is possible to control their size and their shape by adjusting the deposition conditions (substrate temperature, saturated atmosphere...)^{28,29}. From the depth of the "supra" crystal, the number of monolayers stacked on each other is around 1000. Their crystalline structures were studied by small angle X-Ray reflectivity measurements^{28,29}. The "supra" crystals appear to be made of the best compact stacking of silver nanocrystal monolayers such as FCC or HCP structures. Figures 4B, 4C and 4D show that similar "supra" crystals are produced by replacing HOPG by gold, silicon and $\text{Al}_{0.7}\text{Ga}_{0.3}\text{As}$, respectively. X-Ray diffraction measurements show reflectograms similar to those observed with HOPG and characteristic of a compact structure. From these data, it is reasonable to conclude that with $\text{Al}_{0.7}\text{Ga}_{0.3}\text{As}$ as substrate, compact monolayers made of nanocrystals are formed. Hence, for any substrate used in the present paper, a compact film made of 5-nm nanocrystals is produced. Fig. 3C shows a partial monolayer. However, for a large amount of nanocrystals "supra" crystals are formed (Fig. 4C). This indicates that compact layer can be formed. The lacks, observed on Fig. 3C are probably due to the fact that not enough nanocrystals were deposited. Nevertheless, the vacancies in the film organization introduce only a minor correction of the reflectivity intensity because the total signal is mainly due to the islands made of densely packed particles.

V. RESULTS AND DISCUSSION

The reflectivity spectra of 5-nm silver nanocrystals organized in hexagonal networks on various substrates such as HOPG, gold, silicon and $\text{Al}_{0.7}\text{Ga}_{0.3}\text{As}$ are presented in Figures 5 and 6.

Under s-polarized light, the reflectivity spectra are recorded at various angles and are found to be similar for all incidence angles. Figure 5 (dotted line) shows the reflectivity spectra recorded at 60° .

Under p polarization, the reflectivity spectra markedly change with the incidence angle (Fig. 6). At a low angle (20°), the reflectivity spectra are similar to those obtained under s polarization (dotted line). This is due to the fact that under s and p polarization at low incidence angles, the electric field vector along the particle film is predominant. At high incidence angles, the perpendicular electric field component becomes much larger than the parallel one.

These spectra lead to several comments:

i) A similar trend in the p polarized spectra recorded at 60° for all substrates is observed with appearance of two maxima around 2.5 eV-3 eV and 3.8 eV-3.9 eV. The latter maximum is more or less marked and depends on the substrate. A minimum at 3.4 eV-3.5 eV is observed. The major difference in the reflectivity spectra shown in Figure 6 is the presence of a minimum at low energy ($E < 3\text{eV}$) or HOPG and gold whereas a plateau is observed with silicon and there is an increase in the reflectivity with $\text{Al}_{0.7}\text{Ga}_{0.3}\text{As}$. Table 1 shows the maxima and the minima of the reflectivity spectra of a film of nanocrystals deposited on the four different substrates.

ii) Under p polarization, as expected, the reflectivity spectra markedly change with the incidence angle. At low angles, the first extremum remains at the same energy. However around 3.4 eV-3.5 eV, a minimum progressively appears (Fig. 6). Above 4 eV, the decay slope remains the same at various incidence angles.

By using the model described above, the calculated reflectivity spectra corresponding to s and p polarizations at various incidence angles and on various substrates are deduced:

The reflectivity spectrum calculated at 60° (solid line) under s polarization is shown in Figure 5. It is similar to those observed experimentally (dotted lines). Under p polarization, the calculated reflectivity spectra at various incidence angles are shown in Figure 7. An increase in the minimum at 3.4-3.5 eV on increasing the incidence angle is observed.

The general trend of calculated spectra (under p and s polarization), i.e., the relative intensities of the extrema and the variation of their positions with the nature of the substrate (Table 1) remain

similar to those obtained experimentally (Fig. 6). As stated above, under s-polarization, the electric field vector does not provide any information on the optical surface anisotropy.

For a given substrate, the experimental spectra in Figure 6 show rather good agreement with that calculated (Fig. 7). However some differences are observed:

i) The experimental spectra are broader and their intensities lower than those obtained from calculations. This can be explained by the fact that silver nanocrystals are coated with dodecanthiol inducing damping and broadening of the resonance plasmon peak⁴⁻⁶. Furthermore, it is well known that the plasmon resonance and its bandwidth markedly change with the particle size^{2,26,30}. The nanocrystal sizes involved in the film (monolayer in a hexagonal network) are not monodispersed as used in the model. They are characterized by a size distribution of 13%. These features (coating and size distribution) easily explain the broadening of the experimental spectra compared to that calculated.

ii) Figure 6 shows a peak at high energy (3.8 eV-3.9 eV) which is not obtained by calculation (Fig. 7). To understand these differences in the reflectivity spectra, a rough approximation is made: Let us assume the reflectivity spectra under s polarization (Fig. 5) and p polarization at a low incidence angle (dotted line Figure 6) are equivalent. That is to say, the electric field vector is always directed along the film direction (parallel to the substrate). At a large incidence angle (60°), the perpendicular electric field component becomes much larger than the parallel one. The difference between the reflectivity under p and s polarization at 60° would mainly represent the anisotropy of the system and thus, no peak at high energy (3.8 eV-3.9 eV) is observed. This is due to the fact that the slope above 4 eV is similar in both spectra. It is concluded that the high-energy peak (3.8 eV-3.9 eV) cannot be attributed to a plasmon resonance. It is rather difficult to explain the origin of the decay above 4 eV in the reflectivity spectra. It could be due to the interband transition becoming appreciable at 4 eV (the sensitivity of the equipment was carefully tested above 4 eV). The position of the plasmon resonance at low energy cannot be deduced from this rough approximation because the first two extrema appear under both polarizations.

iii) A minimum appears at 3.4 eV-3.5 eV and increases with the incidence angle and is attributed to a plasmon resonance, specific to p polarization. This is well confirmed by calculation.

The experimental and calculated spectra of the nanocrystal film deposited on various substrates change markedly. The reflectivities due to the substrate and the film made of nanocrystals are both non-negligible. The overall reflectivity spectrum is the sum of both contributions: the reflectivity of the nanocrystals monolayer and that of the substrate averaged by the absorption of the

nanocrystal monolayer. It is thus not surprising that optical spectra differ with the substrate and this is related to its refractive index (Figs. 6 and 7).

The model used above is limited to dipole-dipole interactions. In fact, the substrate could influence the optical response of the silver nanocrystal monolayer by image forces, i.e., formation of image dipoles in the substrate induced by the dipoles in the nanocrystals, subjected to an electromagnetic field. To introduce the image forces, the Barrera calculations described in reference [14] are used. The calculated spectra are very similar to those obtained without image forces (Fig.7). This result is explained by the fact that the silver nanocrystals are not in direct contact with the substrate. Thus the dipole/image-dipole distance is sufficiently high for this term to be negligible.

A more complete program, which takes into account the multipolar effects, is available^{13,31,32}. This program was adapted to calculate the reflectivity of the system. The spectra obtained are, once more, very similar to the spectra calculated with a simple model. The multipolar effects are not important in this system because the nanocrystals are small and are separated by a large distance (2 nm), and dipolar approximation seem to be sufficient to describe experimental data.

Hence with or without image forces and multipolar interactions, the calculated reflectivity spectra of the nanocrystals film deposited on a substrate of dielectric constant $\varepsilon_{sub} = (5; 7)$ (similar that of the HOPG between 2 and 3.8 eV) are mainly the same as shown in Figure 8. One question arises: Does the use of the classical 3D Maxwell-Garnett³³ theory change the reflectivity spectra of 2D film made of nanocrystals? We have to point out that this model is used in the stratified media theory of Abelès, which takes into account the dimensionality of the film. Very surprisingly this model gives results similar to those used for a film (Fig. 8). The invariance in the calculated reflectivity spectra as shown in Figure 8 are obtained for the various substrates used. Hence the three theories qualitatively explain the experimental spectra, i.e. the extrema are at the same position.

From these data, it is concluded that the influence of the substrate on the optical response is mainly due to its intrinsic optical property, by the way of its refractive index.

VI. CONCLUSION

Reflectivity measurements on silver nanocrystals, deposited on various substrates, are presented. From experimental and calculated spectra, it is concluded that the major change in the responses is due to the refractive index of the substrate. Indeed, the nanocrystal film is far enough from the substrate to neglect the influence of the image forces. Thus, the positions of the two

plasmon resonances, characteristic of the film optical anisotropy, do not depend on the nature of the substrate. Hence, they can be identified from the reflectivity spectrum, by the calculations. These results can be generalized to various substrates, especially to absorbing ones, whose optical response is not obvious. The film optical characteristics are due in part to the dipolar interactions between nanocrystals, which induce appearance of a plasmon resonance at high energy indicative of collective optical properties.

Acknowledgments

The authors gratefully thank Dr A. Taleb from our laboratory and Dr. F. Vallée (CPMOH Bordeaux) for fruitful discussions, and Dr. F. Charra (SRSIM, CEA, Saclay) for providing the gold support and STM experiments, Professor R. Carles (LPST, Toulouse), for providing the $\text{Al}_{0.7}\text{Ga}_{0.3}\text{As}$ support and Dr. D. Mariolle (LETI, CEA, Saclay) for SEM visualization on silicon substrates.

* Electronic address: pileni@sri.jussieu.fr; URL: <http://www.sri.jussieu.fr>

- ¹ J. A. Creighton and D. G. Eadon, *J. Chem. Soc. Faraday Trans.* **87**, 3881 (1991)
- ² U. Kreibig and C. V. Fragstein, *Z. Physik* **224**, 307 (1969)
- ³ H. Able, K. P. Charle, B. Tesche and W Schulz,e *Chem. Phys.* **68**, 137 (1982)
- ⁴ H. Hovel, S. Fritz, A. Hilger and U. Kreibig, *Phys.Rev.B* **48**, 18178 (1999)
- ⁵ Persoon, *Surface Science* **281**, 153 (1993)
- ⁶ K. P. Charle, F. Frank and W. Schulze, *Ber Bunsenges. Phys.Chem* **88**, 350 (1984)
- ⁷ N. Nilius, N. Ernst and H. J. Freund, *Phys. Rev. Lett.* **84**, 84 (2000)
- ⁸ N. Nilius, N. Ernst and H. J. Freund, *Surf. Sci.* **478**, 1327 (2001)
- ⁹ T. Wendzel, J. Bosbach, F. Stiez and F. Trager, *Surf. Sci.* **432**, 257 (1999)
- ¹⁰ D. Martin, J. Jupille and Y. Borenszstein *Surf. Sci.* **402**, 433 (1998)
- ¹¹ T. Yamaguchi, S. Yoshida and A. Kinbara *Thin Solid Films* **21**, 173 (1974)
- ¹² I. Simonsen, R. Lazzari, J. Jupille, S. Roux, *Phys. Rev. B* **61**, 7722, (2000)
- ¹³ A. Modinos, V. Yannopapas, N. Stefanou, *Phys. Rev. B* **61**, 8099 (2000)
- ¹⁴ R. G. Barrera, M. del Castillo-Mussot, G. Monsivais, P. Villasenor, W. L. Mochan, *Phys. Rev. B* **43**,

13819 (1991)

- 15 G.C. Schatz *Theochem* **573**, 73 (1995)
- 16 P. Royer, J.P. Goudonnet, R.J. Warmack and T.L. Ferrell, *Phys. Rev. B* ,**35**, 3753 (1993)
- 17 R. Lazzari, J. Jupille, Y. Borensztein, *Appl. Surf. Sci.* **142**, 451 (1999)
- 18 A. Taleb, C. Petit, M. P. Pileni *Chem. Mat.* **9**, 950 (1997)
- 19 C. Petit, A. Taleb, M. P. Pileni, *J. Phys. Chem. B* **103**, 1805 (1999)
- 20 V. Russier, M. P. Pileni, *Surf. Sci.* **425**, 313 (1999)
- 21 A. Taleb, V. Russier, A. Courty, M. P. Pileni, *Phys. Rev. B* **59**, 13350 (1999)
- 22 *Solid State Physics* N. W. Ashcroft and N. D. Mermin (Holt Saunders International Editions, 1976)
- 23 *Handbook of optical constants of solids, vol. I* E. D. Palik, (Academic Press, 1985)
- 24 F. Abelès, *Annales de Physique* **5**, 596 (1950)
- 25 *Theory of reflection* J. Lekner, (Martinus Nijhoff Publishers, Dordrecht, 1987)
- 26 M. P. Pileni, *J. Phys. Chem.* **97**, 6961 (1993)
- 27 C. Petit, P. Lixon, M. P. Pileni *J. Phys. Chem.* **97**, 12974 (1993)
- 28 A. Courty, C. Fermon, M. P. Pileni, *Adv. Mat.* **13**, 254 (2001)
- 29 A. Courty, O. Araspin, C. Fermon, M. P. Pileni, *Langmuir* **17**, 1372 (2001)
- 30 *Optical Properties of Metal Cluster* U. Kreibig, M. Vollmer (ed. Springer, 1993)
- 31 N. Stefanou, V. Yannopapas, A. Modinos, *Comput. Phys. Commun.* **113**, 48 (1998)
- 32 N. Stefanou, A. Modinos, *J. Phys: Cond. Mat.* **5**, 8859 (1993)
- 33 J. C. Maxwell-Garnett, *Philos. Trans. R. Soc. Lond.* **203**, 385 (1904)

Figures

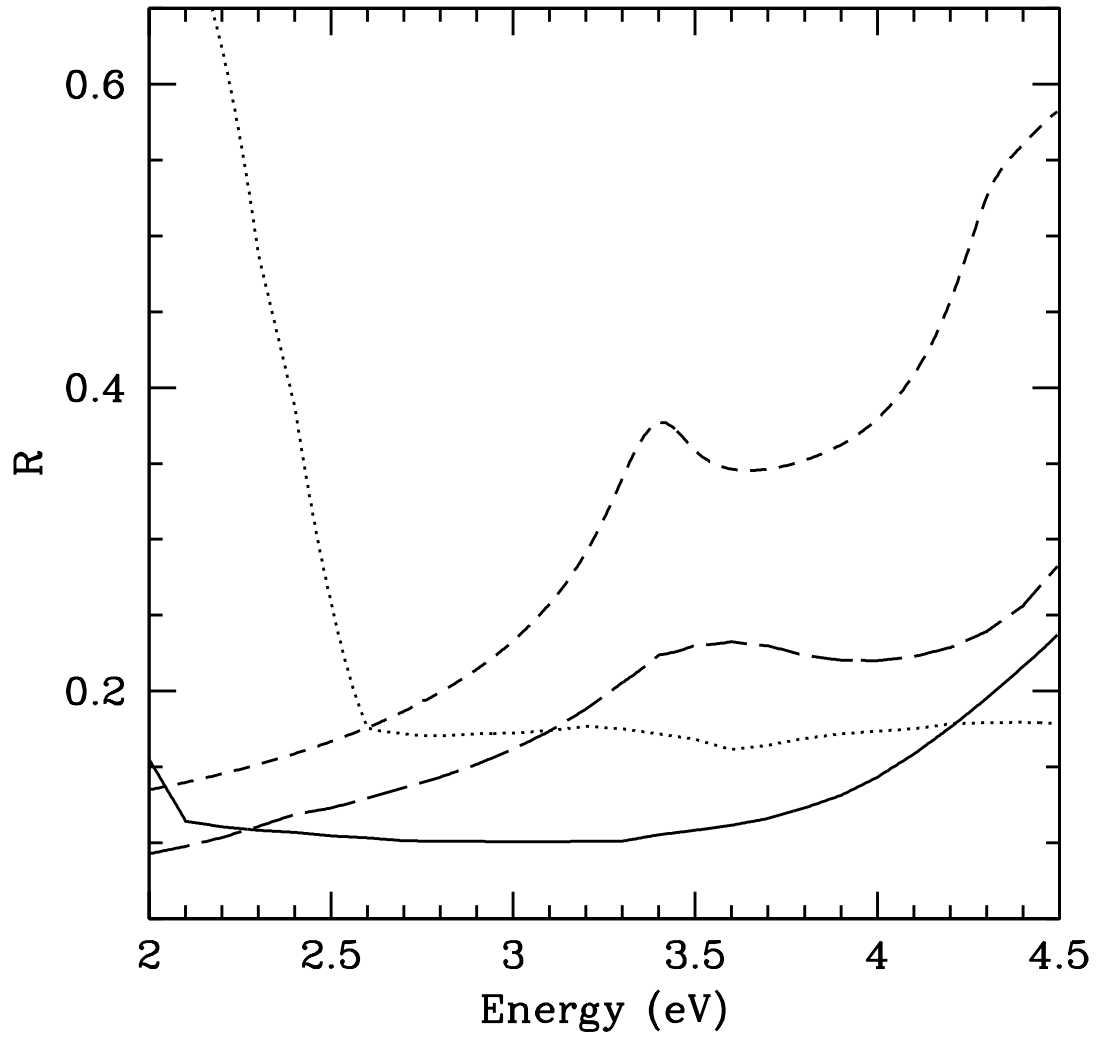


FIG. 1: Calculated reflectivity spectra of the bare substrates: HOPG (solid line), silicon (short dashed line), AlGaAs (long dashed line) and Au (dots)

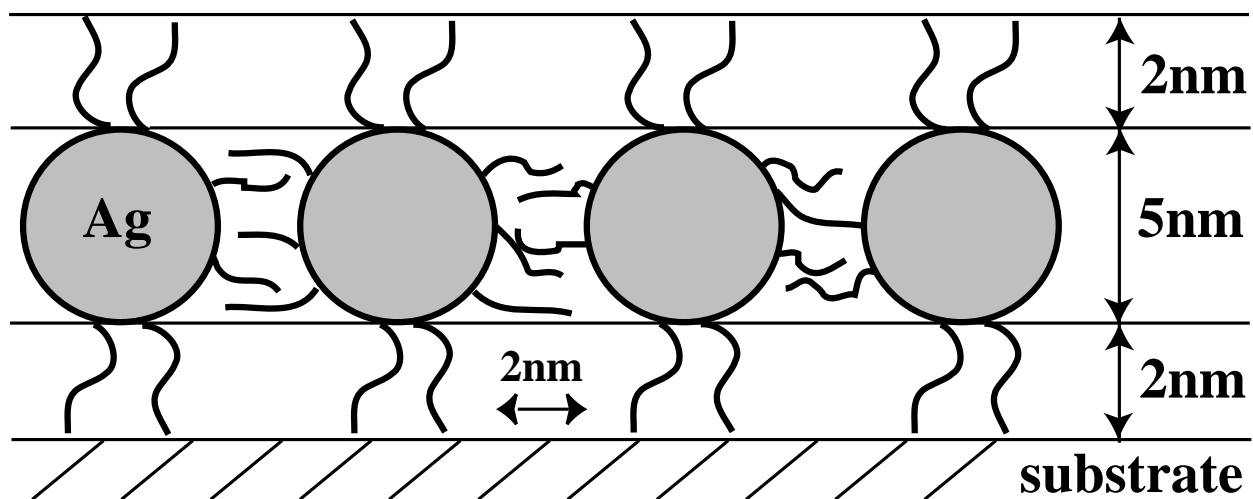


FIG. 2: Schematic representation of the modeled system

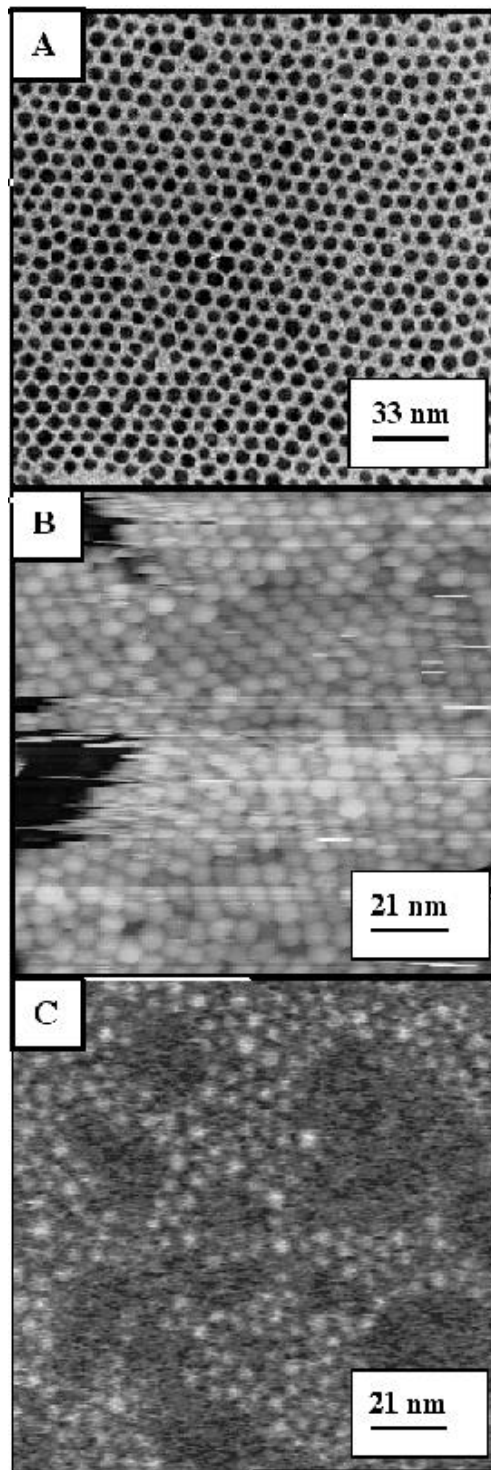


FIG. 3: Monolayer of 5-nm silver nanocrystals on HOPG (A), Au (111) (B) and silicon (C). These images were obtained by TEM in A, constant current mode STM ($V_t=2.5$ V, $I_t=0.8$ nA) in B and by SEM in C.

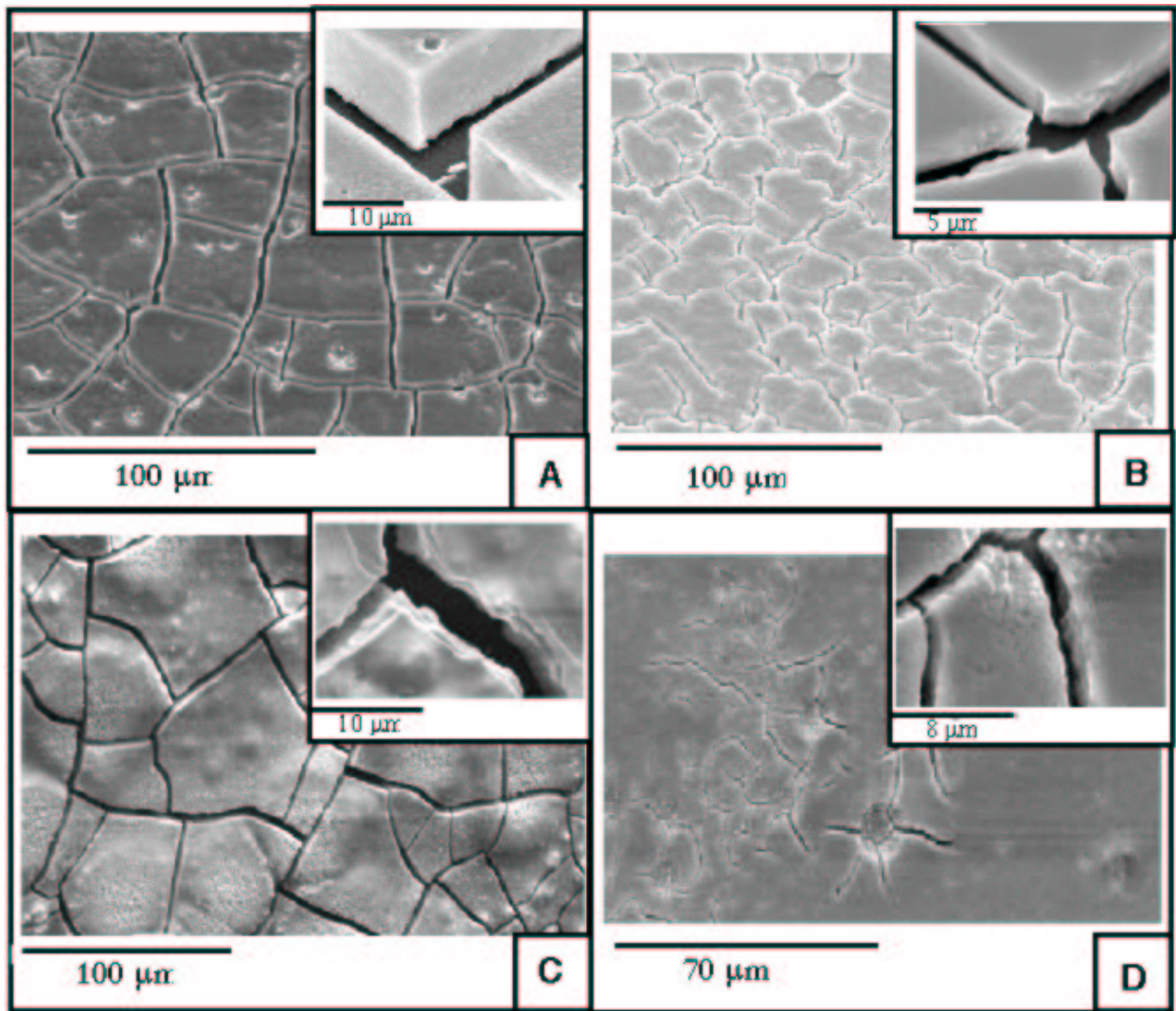


FIG. 4: SEM images obtained from different substrates immersed in 200 μl of a highly concentrated colloidal silver solution ($3 \cdot 10^{-6}$ mol/l) and dried for 9 h under a hexane vapor atmosphere. HOPG (A), silicon (B), AlGaAs (C) and Au (D) substrates were used.

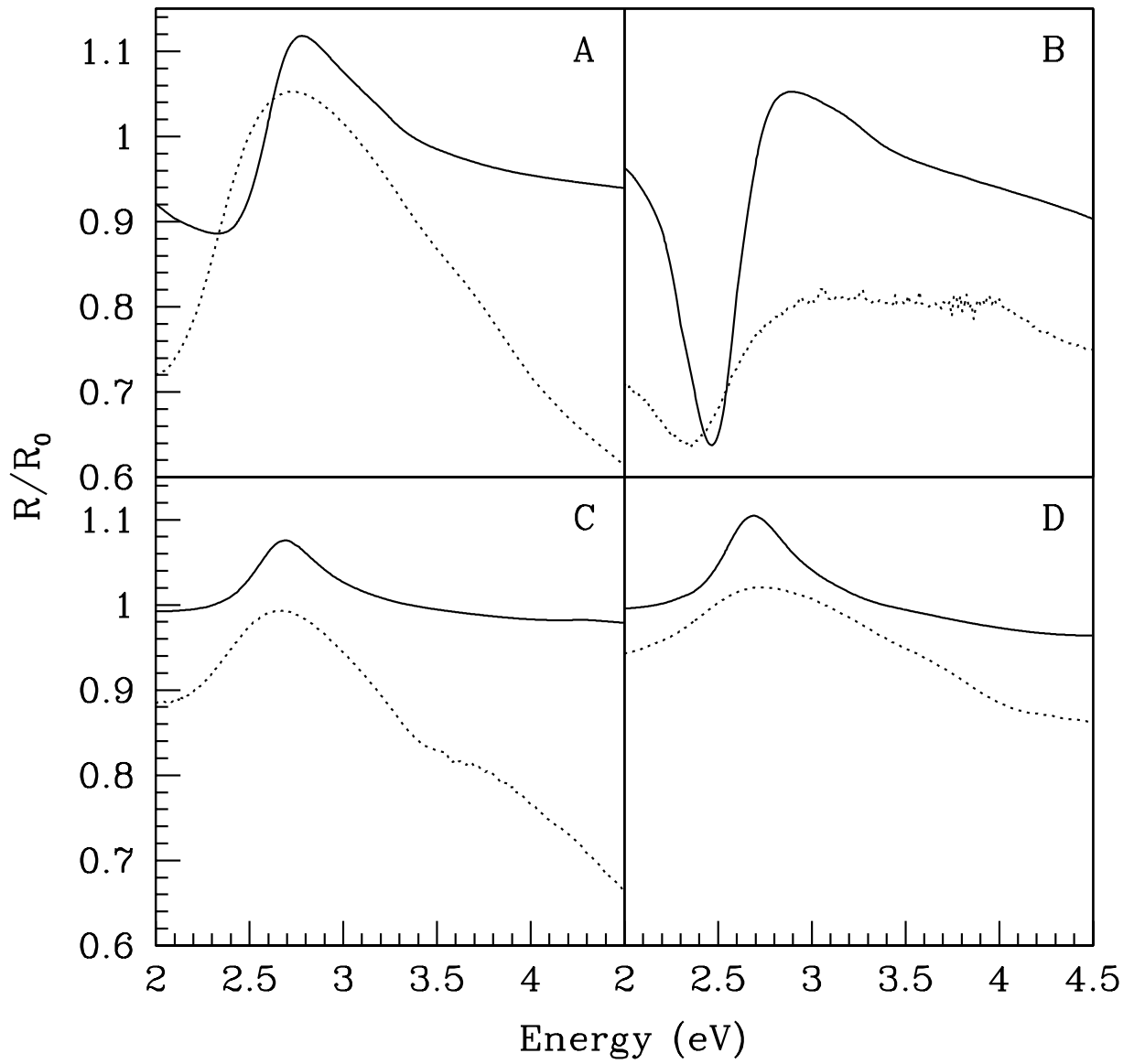


FIG. 5: Experimental (dotted line), calculated (solid line) reflectivity spectra of silver nanoparticle monolayer on HOPG (A), gold (B), silicon (C), $\text{Al}_{0.7}\text{Ga}_{0.3}\text{As}$ (D) with s-polarized light and at a 60° incidence angle.

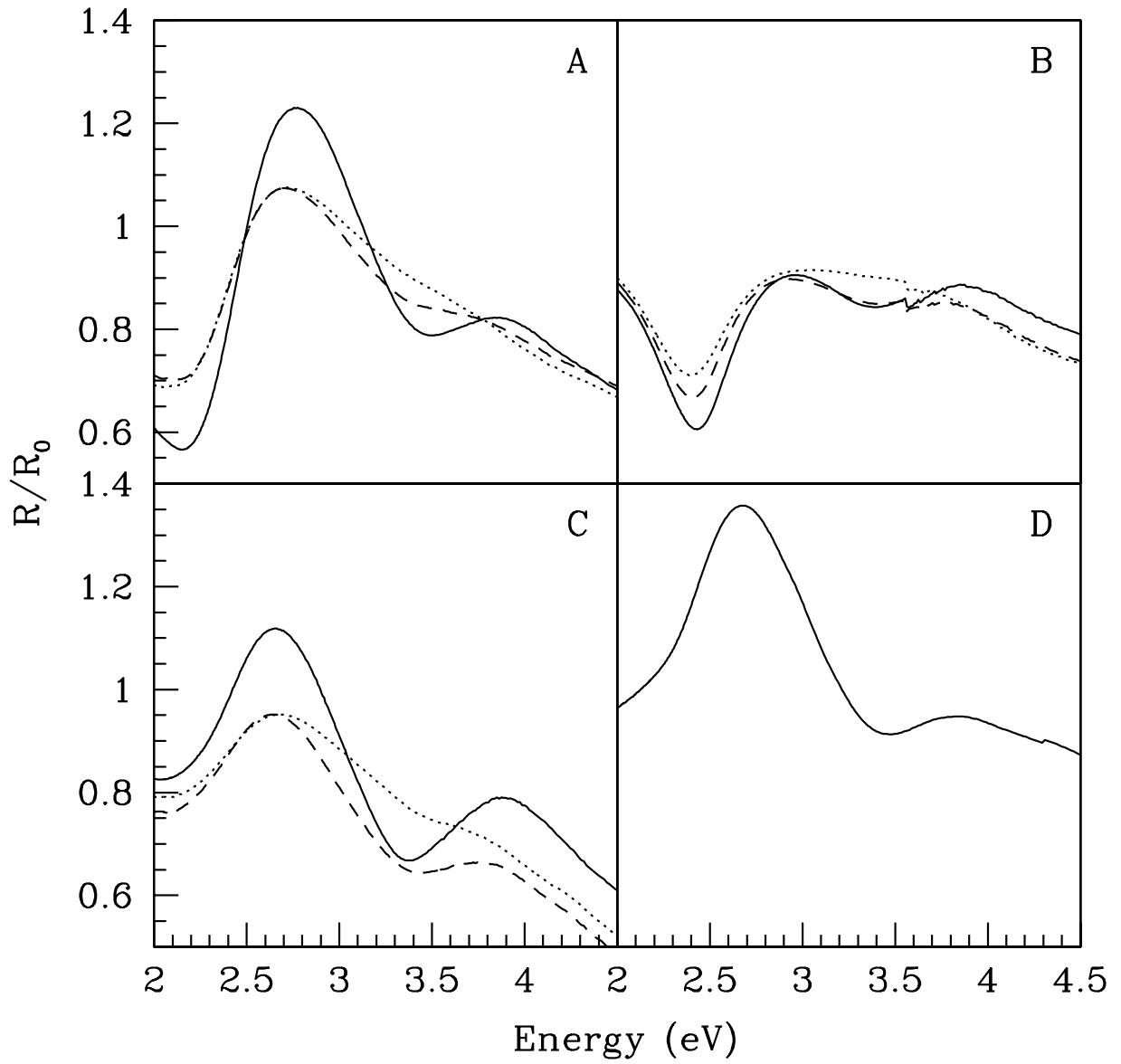


FIG. 6: Experimental reflectivity spectra of silver nanoparticles monolayer on HOPG (A), gold (B), silicon (C), $\text{Al}_{0.7}\text{Ga}_{0.3}\text{As}$ (D) under p-polarized light and at incidence angles of 60° (solid line), 45° (dashed line), 20° (dotted line).

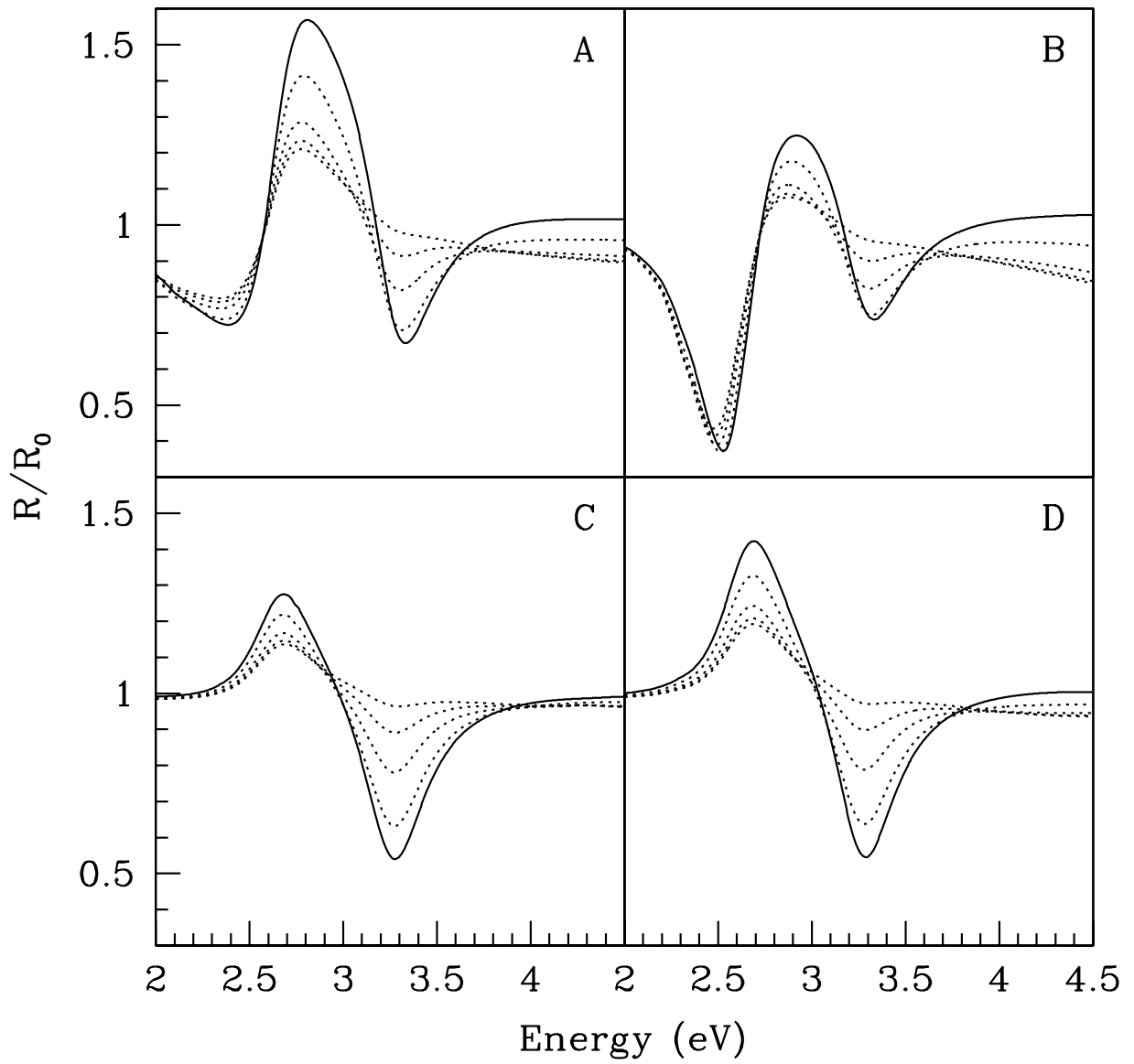


FIG. 7: Calculated reflectivity spectra of silver nanoparticles monolayer on HOPG (A), gold (B), silicon (C), $\text{Al}_{0.7}\text{Ga}_{0.3}\text{As}$ (D) with p-polarized light and at incidence angles of 60° (solid line), 50° , 40° , 30° , 17° (dotted lines)

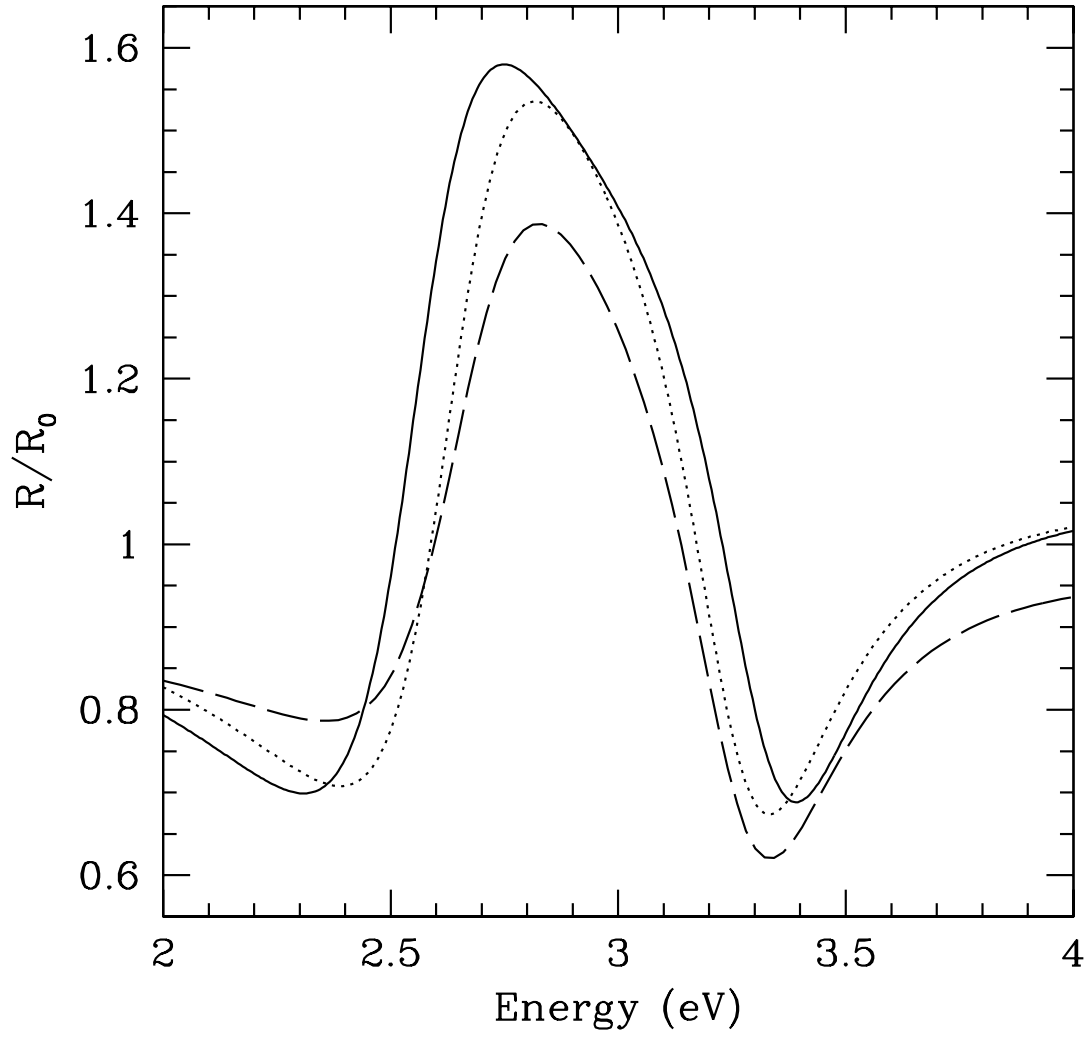


FIG. 8: Calculated reflectivity spectra of silver nanoparticles monolayer on a substrate of dielectric constant $\epsilon_{sub} = (5; 7)$ for the 3 models: Maxwell-Garnett³³ (solid line), Barrera¹⁴ (dotted line), Stefanou³¹ (dashed line)

Tables

Extrema	1st min		1st max		2nd min		2nd max	
	Ex	Th	Ex	Th	Ex	Th	Ex	Th
HOPG	2.15	2.38	2.83	2.80	3.50	3.34	3.86	/
Gold	2.4	2.52	3.0	2.92	3.4	3.34	3.86	/
Silicon	/	/	2.65	2.68	3.38	3.28	3.87	/
AlGaAs	/	/	2.68	2.68	3.47	3.30	3.85	/

TABLE I: Maxima and minima of the reflectivity spectra recorded under p polarization at fixed incidence angle (60°) on various substrates.